REPORT DOCUMENTATION PAGE

Form Approved
OMB No. 0704-0188

1. REPORT DATE *(DD-MM-YYYY)*	2. REPORT TYPE	3. DATES COVERED *(From - To)*
03/03/2006	Final	2004

4. TITLE AND SUBTITLE
Bistatic Synthetic Aperture Sonar Measurements and Preliminary Analysis

5a. CONTRACT NUMBER
N00014-02-G-0460

5b. GRANT NUMBER

5c. PROGRAM ELEMENT NUMBER

6. AUTHOR(S)
Steven G. Kargl, Kevin L. Williams, Eric L. Thoros, Joseph L. Lopes

5d. PROJECT NUMBER

5e. TASK NUMBER
0033

5f. WORK UNIT NUMBER

7. PERFORMING ORGANIZATION NAME(S) AND ADDRESS(ES)
Applied Physics Laboratory
University of Washington
1013 NE 40th ST
Seattle WA 98105-6698

8. PERFORMING ORGANIZATION REPORT NUMBER

9. SPONSORING/MONITORING AGENCY NAME(S) AND ADDRESS(ES)
Office of Naval Research
875 N. Randolph St., Suite 1425
Arlington, VA 22203-1995

10. SPONSOR/MONITOR'S ACRONYM(S)

11. SPONSOR/MONITOR'S REPORT NUMBER(S)

12. DISTRIBUTION/AVAILABILITY STATEMENT
Approved for public release; distribution unlimited.

13. SUPPLEMENTARY NOTES
Published in "Proceedings of Boundary Influences in High Frequency Shallow Water Acoustics" held University of Bath, UK, 5-9 September 2005. Joint government work. Includes color plates.

14. ABSTRACT

As part of the sediment acoustics experiment-2004 (SAX04), bistatic synthetic aperture sonar (SAS) measurements were made. The Applied Physics Laboratory (APL-UW) rail/tower system was used to receive signals emitted by either the Naval Surface Warfare Center-Panama City (NSWC-PC) tower with a parametric source or a separate APL-UW tower with an omnidirectional source. For the parametric source, the relevant frequency bands are 1-5 and 60-65 kHz. The omnidirectional source emitted a shore 20 kHz sine wave burst. A brief description of the measurement geometry will given, and the time-domain imaging algorithm will be outlined.

The NAVSEA funding document title for N00014-02-G-0460 is "SAX04 Bistatic Measurements of VLF Bottom Reverberation and Target Strength.."

15. SUBJECT TERMS

16. SECURITY CLASSIFICATION OF:			17. LIMITATION OF ABSTRACT	18. NUMBER OF PAGES	19a. NAME OF RESPONSIBLE PERSON
a. REPORT	b. ABSTRACT	c. THIS PAGE			Robert Headrick
UU	UU	UU	UU		19b. TELEPHONE NUMBER *(Include area code)*

Final Report

SWAMSI – Bistatic scattering measurements on mine-like targets during SAX04

Contract #: N00014-01-G-0460, Task Order #33

Principal Investigators: Kevin L. Williams, Eric Thorsos

Applied Physics Laboratory
University of Washington
1013 NE 40th St
Seattle, WA 98105-6698

E-mail: williams@apl.washington.edu (Williams)
Phone: 206-543-3949 (Williams), 206-543-1369 (Thorsos)
Fax: 206-543-6785

SUMMARY:

As part of the sediment acoustics experiment-2004 (SAX04), bistatic synthetic aperture sonar (SAS) measurements were made. The Applied Physics Laboratory (APL-UW) rail/tower system was used to receive signals emitted by either the Naval Surface Warfare Center-Panama City (NSWC-PC) tower with a parametric source or a separate APL-UW tower with an omnidirectional source. For the parametric source, the relevant frequency bands are 1-5 and 60-65 kHz. The omnidirectional source emitted a short 20 kHz sine wave burst. The resulting data has been preprocessed into matrix form and is available for further analysis by other researchers.

In addition, we have presented the results of our analysis to date of this same data in two publications:

S. G. Kargl, K. L. Williams, E. I. Thorsos, J. L. Lopes, "Bistatic synthetic aperture sonar measurements and preliminary analysis." in *Proceedings of Boundary Influences in High Frequency, Shallow Water Acoustics*, University of Bath, UK 5th-9th September 2005. (Copy attached as part of this final report)

K. L. Williams, E. I. Thorsos, S. G. Kargl, D. Tang, J. L. Lopes and C. L. Nesbitt, "Synthetic Aperture Sonar Measurements of Bistatic and Monostatic Scattering from Proud and Buried Targets" submitted to JUA(USN).

BISTATIC SYNTHETIC APERTURE SONAR MEASUREMENTS AND PRELIMINARY ANALYSIS

STEVEN G. KARGL, KEVIN L. WILLIAMS, ERIC I. THORSOS

Applied Physics Laboratory, University of Washington, 1013 NE 40th St., Seattle WA 98105. Email: Kargl@apl.washington.edu

JOSEPH L. LOPES

Naval Surface Warfare Center-Panama City, 110 Vernon Ave., Panama City FL 32407

As part of the sediment acoustics experiment-2004 (SAX04), bistatic synthetic aperture sonar (SAS) measurements were made. The Applied Physics Laboratory (APL-UW) rail/tower system was used to receive signals emitted by either the Naval Surface Warfare Center-Panama City (NSWC-PC) tower with a parametric source or a separate APL-UW tower with an omnidirectional source. For the parametric source, the relevant frequency bands are 1-5 and 60-65 kHz. The omnidirectional source emitted a short 20 kHz sine wave burst. A brief description of the measurement geometry will be given, and the time-domain imaging algorithm will be outlined. An important aspect of these measurements is the fixed location of the source towers relative to the rail/tower system removes possible problems with motion compensation of source and receiver arrays as could occur when the arrays are mounted on autonomous underwater vehicles. Various objects were placed in the field of view of the SAS system. Imaging results for one of these objects will be shown.

1 Introduction

A bistatic synthetic aperture sonar (SAS) scenario, which utilizes multiple autonomous underwater vehicles (AUV), has the desirable features of possible rapid high-area coverage, multiple aspect angle looks at an object (e.g., forward scattering), and covert operation. Unfortunately, these features are achieved at the expense of relative vehicle motion. Traditional towed SAS systems have implemented motion compensation schemes where the source and receiver are mounted on the same vehicle. In the multi-AUV, bistatic SAS scenario, not only is motion compensation for each AUV required, but each AUV must register its position with all other AUV positions. This is required because coherent processing of the recorded signals needs proper phase information to form images.

In this paper, the problems with the use of AUVs are removed, so that we can concentrate on the multiple aspect angle looks at an object. The APL-UW rail system [1] with its SAS array is used in a receive mode while the source is located on a distant, fixed, tower. The APL-UW mobile tower [2] and NSWC-PC parametric sonar tower [3] transmitters were used in a set of experiments during SAX04. This paper describes the

measurements and demonstrates that the resulting pulse compressed baseband signals and the bistatic SAS images made using these signals yield additional information for the detection and classification of targets.

2 Experimental Configuration

Figure 1 depicts the bistatic configuration of the SAX04 experiments. Several targets were placed on the seafloor 10 meters from the source tower. For the measurements with the NSWC-PC parametric source, the acoustic axis of the transmitter was aligned through (or nearly through) the proud target. The parametric source was driven with two linear frequency modulated (LFM) chirps where the primary carrier frequencies were nominally 61 and 64 kHz with a 2 kHz bandwidth and 4 ms duration. One chirp had a positive chirp rate while the chirp rate of the second was negative. The generated secondary field has an approximate frequency range of 1-5 kHz. A second set of LFM chirps generated a secondary field with a 5-16 kHz range where the carrier frequencies were nominally 57 and 67 kHz with a 7.5 kHz bandwidth.

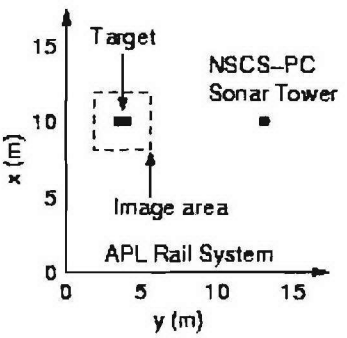

Figure 1. The rail is located along the y axis and signals were recorded from −13.5 to 13.5 m at a $\Delta y = 0.025$ m interval. This interval was chosen because the horizontal aperture of the receiver is $d_h = 0.1$ m, and Gough and Hawkins [4] have suggested that the interval should be $\Delta y = d_h/4$. The dashed box denotes the edge of the images to be shown, and the largest target placed in the center of the image area was approximately 2 m in length.

For the measurements with the parametric source, the NSWC-PC tower's location was (x,y) = (10,13.5) m with the source approximately 4 m above the seafloor. The APL-UW mobile tower had a nominal location of (x,y) = (28,15) m and its omnidirectional source was 4.33 m above the seafloor.

For the measurements that involved the NSWC-PC parametric source, only images of the target from the primary frequency band are shown. Images, based on the secondary field, have been formed, but the low signal-to-noise of the data tends to lower the quality of images. The strength of a parametrically generated field depends on the amplitude of the primary fields. During SAX04, it was found that the direct arrival of the primary field was sufficient to saturate the pre-amplifiers of the APL-UW receiving array. The APL-UW electronics were originally designed for a series of experiments that did not include the bistatic SAS measurement, so bandpass filtering prior to the pre-amplification stage was not needed. The addition of bandpass filtering during the bistatic SAS measurements was not

possible. Thus, the amplitude of the primary fields had to be limited to avoid saturation of the pre-amplifiers. As a consequence, the strength of the secondary fields was also reduced.

3 Time Domain Imaging Algorithm

A time-domain image is constructed via a delay and sum algorithm. For a pixel located at $\mathbf{r}_{ij} = (x_i, y_j, 0)$, the complex image amplitude is

$$p_{ij} = p(\mathbf{r}_{ij}) = \sum_k A(\mathbf{r}_s, \mathbf{r}_{rk}, \mathbf{r}_{ij})\, p(y_{rk}, t_k) \exp[-ik_0(R_s + R_{rk})] \qquad (1)$$ where

$t_k = (R_S + R_{rk})/c$ is the time delay for propagation from the source to the pixel and then from the pixel to the receiver. The separation distances are $R_S = |\mathbf{r}_S - \mathbf{r}_{ij}|$ and $R_{rk} = |\mathbf{r}_{rk} - \mathbf{r}_{ij}|$ where $\mathbf{r}_S$ and $\mathbf{r}_{rk}$ are the source and receiver locations and $\mathbf{r}_{ij}$ is the pixel location on the mean sediment surface z = 0, and the speed of sound in the water is c = 1538 m/s. The amplitude factor, $A(\mathbf{r}_s, \mathbf{r}_{rk}, \mathbf{r}_{ij})$, contains the beam patterns of the source and receiver as well as a time varying gain to enhance the contrast across an image. In the formation of the images in Sec. 4, contributions that occur outside of the -6 dB down points of the main lobe of the beam patterns are ignored (i.e., suppression of possible interference from side lobes). The complex, pulse-compressed, baseband pressure at the k^{th} receiver location is $p(y_{rk}, t_k)$. Phase factor in Eq. (1), $\exp[-ik_0(R_S + R_{rk})]$, is phase compensation for a spherically diverging wave and the assumed time convention of $\exp(-i\omega t)$ where ω and k_0 are the angular carrier frequency and wavenumber in water, respectively. If the y-axis is aligned with the along-track direction, then the separation distances are

$$R_s = [x_i^2 + (y_j - y_s)^2 + z_s^2]^{1/2}, \quad R_{rk} = [x_i^2 + (y_j - y_{rk})^2 + z_r^2]^{1/2}. \qquad (2)$$ where

the image plane is tacitly assumed to be at z = 0; however, this restriction is not necessary and other image planes can be defined by the obvious change to Eq. (2). It is also noted that Eq. (2) implies that only the receiver moves along the SAS track via the k subscript. To form an image, the discrete representation of the spatial coordinates are

$$x_i = (x_0 - x_L/2) + (i-1)\Delta x, \quad (i = 1, \cdots, N_x) \qquad (3)$$

$$y_j = (y_0 - y_L/2) + (j-1)\Delta y, \quad (j = 1, \cdots, N_y) \qquad (4)$$

$$y_{rk} = y_{r0} + (k-1)\Delta y_r, \quad (k = 1, \cdots, N_r) \qquad (5)$$ where

the center of the image is at (x_0, y_0), the length of the sides of the image are x_L and y_L, and the initial receiver location is y_{r0}.

Inspection of Eqs. (1)–(5) and the discrete nature of the sampled time signals $p(y_{rk}, t_n)$, $(n = 1, \ldots, N_t)$ suggests that t_k seldom coincides with a discrete time point. Thus, the summation in Eq. (1) requires interpolation of the signals. The interpolation has been performed with 6, 12, 24, and 48 point cubic splines, which were constructed on a discrete

time interval containing t_k. Although cubic spline interpolation permitted the construction of an image, a 4 point Lagrange interpolation algorithm was found to be sufficient for image formation and the Lagrange interpolation is more numerically efficient than cubic spline interpolation. For the results presented here, Lagrange interpolation was used. Additionally, the recorded signals were sampled at 1 MHz, and the use of the pulse-compressed baseband representation yields a finely sampled signal, which significantly reduces the potential for numerical round-off errors in computing the interpolated complex pressure.

4 Discussion

Figure 2 shows the magnitude of the pulse-compressed, baseband scattered pressure and the image formed via the time domain algorithm described above. The target is an open-ended cement pipe, which is nominally 1.1 m in length and 0.42 m in diameter. The data were taken on 21 October 2005. In Fig. 2A, the rail system is located at the top of the image and the parametric source is to the right of the image. The earliest arrival that forms a nearly parabolic arc is the direct arrival from the source to the receiver. The next parabolic arc is the first bottom bounce of the source. The bright, broad arc that appears after 13 ms is the scattering from the cement pipe. It is noted that the y = 13.5 and −13.5 m locations are at approximately 45° and 150° with respect to backscattering to the source. As the receiver moves into the near forward scattering region, the direct arrival, bottom bounce, and scattered signal nearly simultaneously

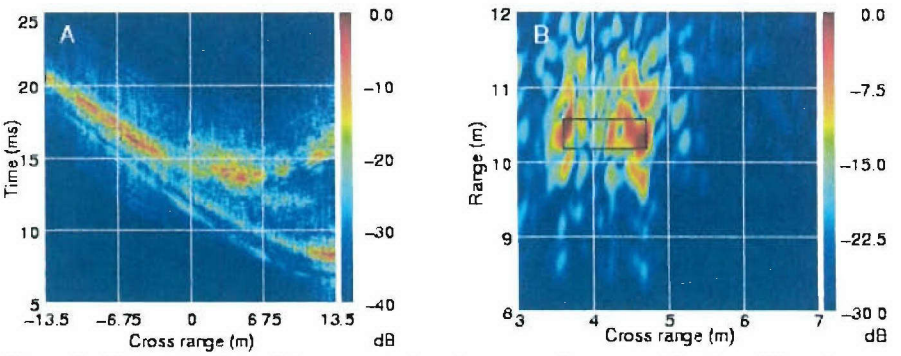

Figure 2. The orientation of the cement pipe gives an end-on ensonification. These images were formed from the LFM chirps of the primary frequencies and each image is normalized to its "hottest" pixel. A. Pulse-compressed baseband signals. B. Bistatic SAS image. The black rectangle represents the nominal dimensions and orientation of the cement pipe.

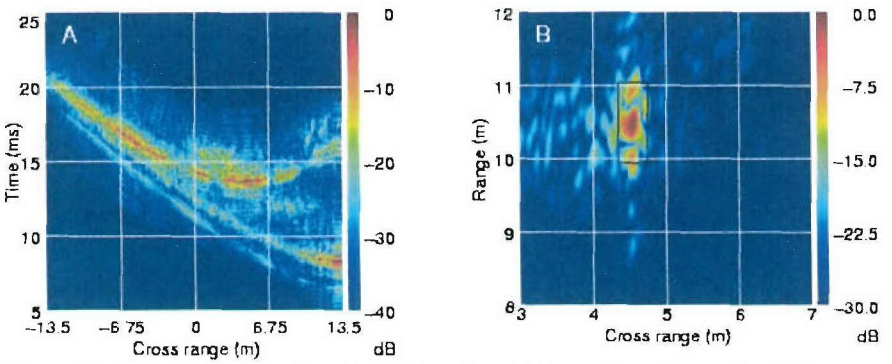

Figure 3. The cement pipe is oriented in a broadside configuration. A. Pulse-compressed baseband signals. B. Bistatic SAS image. The black rectangle represents the nominal dimensions and orientation of the pipe.

reach the receiver. Figure 2B shows the image formed from the data in Fig. 2A. Note, the rail system is located at the bottom of Fig. 2B One can identify the front and back ends of the pipe where the bright feature on the right is nearest the parametric source. The length and width of the pipe can be estimated from this image to be on the order of 1 m long and 0.5 m wide. The spread in the image may be due to multiple scattering of acoustic energy within the open ended pipe.

Figure 3 shows the magnitude of the complex, pulse-compressed, baseband pressure and the image formed from the data. The data were recorded on 22 October 2005. The ends of the pipe are again evident in Fig. 3B at ranges of 10 and 11 m, respectively. However, the brightest feature appears at the center of the pipe. The width of the pipe appears smaller than 0.25 m, which is partly due to the fact that neither end is directly illuminated with sound. As in Fig. 2A, Fig. 3A shows the direct arrival, bottom bounce, and the scattered acoustic signals.

The NSWC-PC parametric source was designed to have a narrow beamwidth for its secondary field, and hence, the primary field also has a narrow beamwidth (i.e., on the order of 5°) [5]. In a bistatic SAS scenario, it may be tempting to light up the underwater environment with an omnidirectional source to obtain high-area coverage. This was carried out with the APL-UW mobile tower on 16 October 2005. A three-cycle 20 kHz sine wave pulse was broadcast from an omnidirectional transducer on the mobile tower with the approximate position of (28,15,4.33) m.

Figure 4 depicts the magnitude of the complex, pulse-compressed, baseband pressure and the image formed from the data. The receiver was moved along the rail at an of interval $\Delta y_r = 0.05$ m. The increased interval was due to limitations in the signal generation for the mobile tower source. The baseband pressure contains four broad parabolic features that span the cross range dimension. These are the direct arrival, the bottom bounce, the surface bounce, and the bottom-surface bounce. With a nominal water depth of 18 m and receiver location of (0,13.5,3.91) m, these arrivals should appear near 18.2, 19.0, 25.7, and 30.7 ms, respectively. The slight discrepancy of the computed arrival times and those observed in Fig. 4A can be attributed to uncertainties in mobile tower location and water depth.

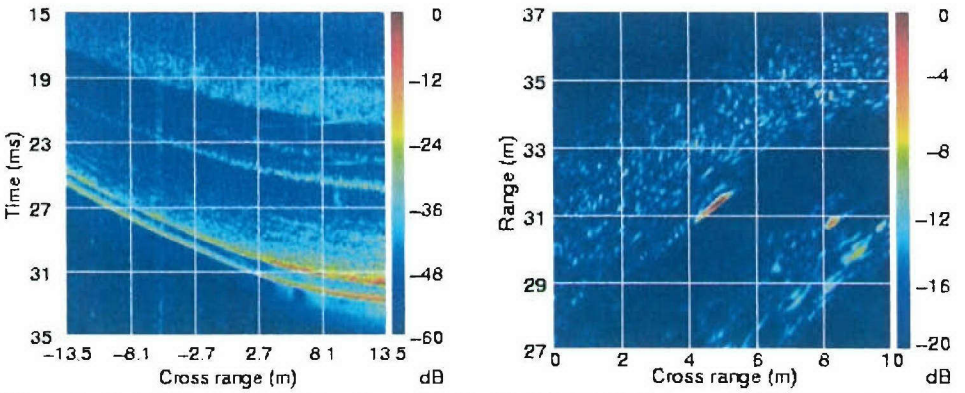

Figure 4. A. Pulse-compressed baseband signals. B. Bistatic SAS image with three targets.

The important features in Fig. 4A are the thin, crescent-shaped arrivals near 25 ms and cross range of 5 to 13.5 m and near 28 ms and cross range of 2 to 13 m. These indicate objects are present, and Fig. 4B reveals at least two targets near (4,31) m and (8,31) m. A third target may be located near (9,30) m. These targets coincide with several proud targets placed on the seafloor for other SAS measurements

5 Conclusions

The combination of a bistatic SAS image and an image of its pulse-compressed baseband data may provide additional information for classification and identification of a target that may not be present in data from conventional monostatic SAS systems. Targets with complex shapes may have low backscattering target strengths, but relatively high bistatic, and in particular, forward scattering cross sections. Inspection of Figs. 2A and 3A shows strong scattering from the cement pipe in the angular range of approximately 90° to 145° with respect to backscattering. The high signal-to-noise ratio provides the possibility of processing schemes to extract elastic responses of the target. Hence, alternative processing schemes may be able to extract this information.

Bistatic SAS images were constructed from data obtained during SAX04. The images in Figs. 2B and 3B clearly indicate the presences of a target and an estimate of its size can be achieved. Even though these images are substantially different due to the orientation of the cement pipe with respect to the source location and rail system, unambiguous identification of the cement pipe from these bistatic SAS images is unlikely. Bistatic SAS images alone may offer advantages over conventional monostatic SAS images for detection due to higher bistatic target strengths. Also, after a target has been detected, the same bistatic data can give important information on classification. Figures 2A and 3A show the magnitudes of the complex, pulse-compressed, baseband pressure. The parabolic arcs associated with scattering from the target in the two orientations are clearly different, and

these may contain target information (e.g., elastic resonances) that is important to classification and identification of the target. SAS processing removes this information.

The complex, pulse-compressed, baseband scattered pressure shown in Fig. 4A for an omnidirectional source clearly demonstrates the need to resolve weak target scattering from multipath arrivals. Otherwise, the signal-to-noise ratio may be too low to adequately resolve a target. For example, a third target may be located at (9,30) m in Fig. 4B. One strategy to achieve high-area coverage would be to have broad horizontal and narrow vertical beams directed at a small depression angle to the surface.

Acknowledgements

This work was supported by the United States Office of Naval Research. The authors thank the crew of the R/V Seward Johnson for their diligence during the SAX04 experiment. We also thank NCSC-PC staff for dock side support during the loading and off-loading of equipment as well as providing a staging area to permit the assembly of the APL-UW rail/tower system. Finally, the bistatic SAS experiment would not have been successful without the tireless effort of the engineers and divers from APL's Ocean Engineering Department.

References

1. Williams K.L., Light R.D., Miller V.W. and Kenney M.F., Bottom mounted rail system for Synthetic Aperture Sonar (SAS) imaging and acoustic scattering strength measurements: Design/operation/preliminary results. *Proceedings of the International Conference "Underwater Acoustic Measurements: Technologies & Results"*, Heraklion, Crete, Greece, 28th June – 1st July 2005.
2. Thorsos E.I., Williams K.L., Chotiros N.P., Christoff J.T., Commander K.W., Greenlaw C.F., Holliday D.V., Jackson D.R., Lopes J.L., McGehee D.E., Richardson M.D., Piper J. and Tang D. An overview of SAX99: Acoustics measurements. *IEEE Journal of Oceanic Engineering* **26**:4-25 (2001).
3. Lopes J.L., Nesbitt C.L., Lim R., Williams, K.L., Thorsos E.I. and Tang D., Subcritical Detection of Targets Buried Under a Rippled Interface: Calibrated Levels and Effects of Large Roughness. *Proceedings of Oceans 2003 MTS/IEEE*, pp. 485-493.
4. Gough P.T. and Hawkins D.W., Unified Framework for Modern Synthetic Aperture Imaging Algorithms. *Int. J. Imag. Sys. Tech.* **8**, 343-358 (1997)
5. Lopes J.L., Nesbitt C.L., Lim R., Williams K.L., Thorsos E.I. and Tang D., Instrumentation Used to Conduct Controlled Measurements of Subcritical Detection of Buried Targets. *Proceedings of the International Conference "Underwater Acoustic Measurements: Technologies & Results"*, Heraklion, Crete, Greece, 28th June – 1st July 2005.